

Novel Canthin-6-one Derivatives: Design, Synthesis, and Their Antiproliferative Activities via Inducing Apoptosis, Deoxyribonucleic Acid Damage, and Ferroptosis

Jinfeng Ding,^{*,||} Tiantian Sun,^{||} Hongmei Wu, Hongwei Zheng, Sijia Wang, Dezhi Wang, Wenpei Shan, Yong Ling,^{*} and Yanan Zhang^{*}



Cite This: *ACS Omega* 2023, 8, 31215–31224



Read Online

ACCESS |



Metrics & More

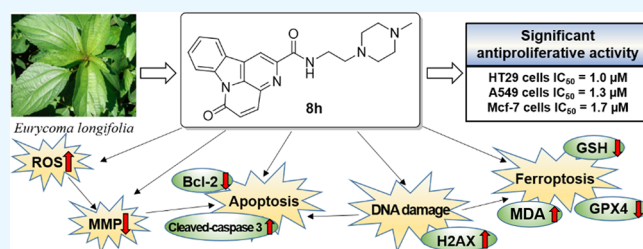


Article Recommendations



Supporting Information

ABSTRACT: A series of novel canthin-6-one (CO) derivatives (8a–l) were designed and synthesized by introducing different amide side chains at the C-2 position, and their water solubility, antiproliferative activity, and preliminary mechanism were investigated. Most compounds displayed high cytotoxicity exhibiting low-micromolar IC₅₀ values against four human cancer cell lines, especially HT29 cells. Meanwhile, the water solubility of active CO derivatives was significantly improved. Among these compounds, compound **8h** with the *N*-methyl piperazine group exhibiting the highest antiproliferative capability with an IC₅₀ value of 1.0 μM against HT29 cells, which was 8.6-fold lower than that of CO. Furthermore, **8h** could upregulate the levels of reactive oxygen species, leading to mitochondrial damage. In addition, **8h** could promote cell apoptosis and DNA damage by regulating the expression of apoptosis-associated proteins (Bcl-2 and cleaved-caspase 3) and the DNA damage-associated protein (H2AX). Most importantly, **8h** also exerted ferroptosis by reducing the GSH level and GPX4 expression as well as increasing the lipid peroxidation level. Thus, the novel CO derivative **8h** with *N*-methylpiperazine represents a promising anticancer candidate and warrants a more intensive study.



1. INTRODUCTION

Cancer is the second general cause of death globally, and the number of cancer cases has also been increasing each year. The main treatment methods for tumors include surgical treatment, radiotherapy, and chemotherapy.^{1,2} Among these modalities, chemotherapy is not only a key player in the treatment of solid tumors but also exhibits a strong efficacy for small invisible metastatic tumors.³ For a long time, natural products are a major source for antitumor drug discovery because of their rich skeleton structure, wide sources, and high medicinal value.⁴ In the past decades, humans have made great achievements in cancer research and treatment by utilizing and modifying natural products.⁵ From the 1940s through the end of 2014, 175 small-molecule drugs were approved for cancer treatment; of them, nearly 75% are of nonsynthetic origin and 49% are directly originated natural products.⁶ Moreover, many natural products undergo only a very small spatial structure or chiral change, but these result in considerable changes in biological activities. Thus, the modification of natural products for enhancing their efficiency and alleviating their toxicity has become a promising and focused research topic.

Canthin-6-one (CO) is a subclass of β -carboline alkaloids and is widely distributed in plants, microorganisms, and marine organisms.^{7–11} CO has broad biological activities, such as antifungal, antibacterial, anti-inflammatory, antiparasite, and

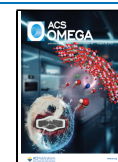
particularly antitumor activities.^{12–20} Moss found that CO extracted and isolated from *Eurycoma longifolia* significantly inhibited the proliferation of breast and lung cancer cells.²¹ In addition, Dekebo et al. found that CO exerts its antiproliferative effect on PC-3, HT29, Jurkat, HeLa, C6, and NIH-3 T3 cells.²² CO could facilitate the incorporation of 5-bromo-2'-deoxyuridine into DNA and inhibit the formation of the mitotic spindle, so as to interfere with G2/M transformation and exert the antiproliferative effect on cancerous cells.²³ This suggested that CO can inhibit the growth of multiple cancer cells by reducing DNA replication and preventing cell mitosis in G2/M, thereby explaining the significant potential application value of CO in cancer treatment.

Unfortunately, CO is associated with the disadvantages of poor water solubility and moderate antiproliferative activity, which limit its clinical application.²⁴ Therefore, modifying the natural product CO to improve the lipid-water partition

Received: May 14, 2023

Accepted: July 26, 2023

Published: August 18, 2023



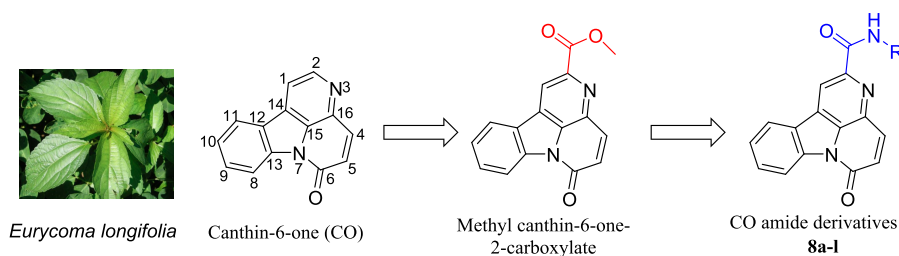
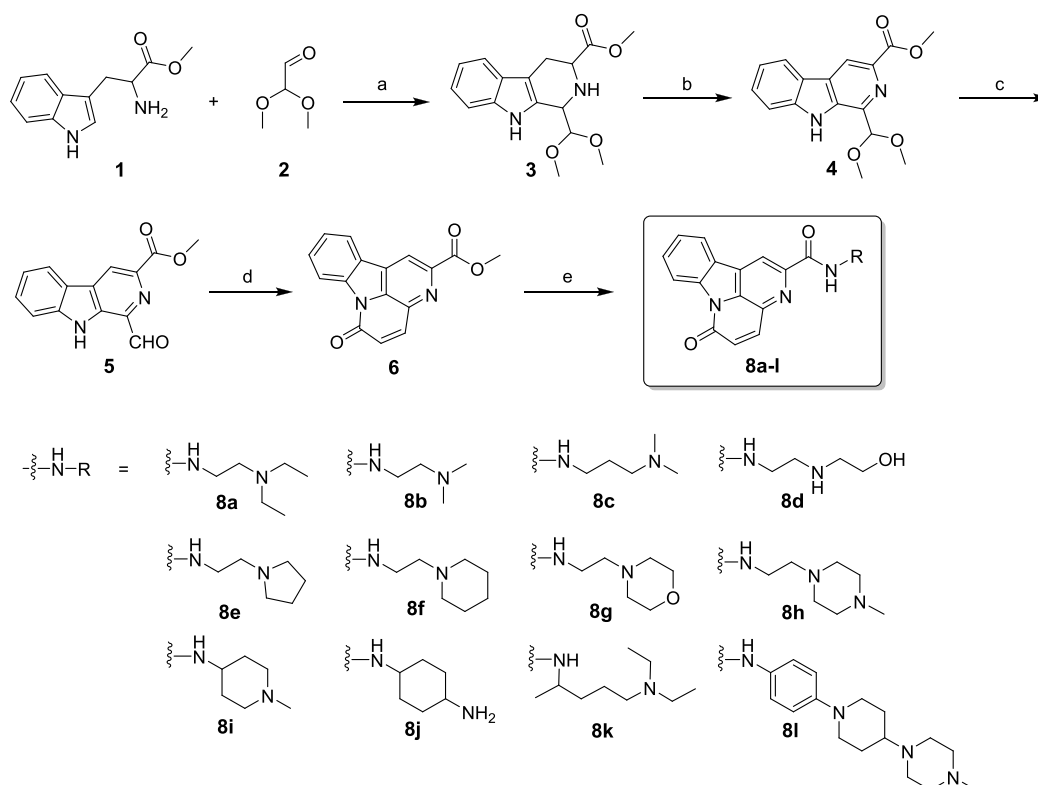


Figure 1. Design strategy of novel CO amide derivatives.

Scheme 1. Chemical Synthesis of 8a–l^a



^aReagents and conditions: (a) CF_3COOH , DCM, rt, 6 h, 90%; (b) KMnO_4 , THF, rt, 12 h, 72%; (c) CH_3COOH , H_2O , 90 °C, 1 h, 95%; (d) acetic anhydride, Na_2CO_3 , 120 °C, 5 h, 80%; (e) different substituted primary amines 8a–l, MeOH, 80 °C, 12 h, 48–78%.

coefficient and antiproliferative activity is of great significance. Therefore, by introducing various hydrophilic nitrogen-containing heterocycles or alkyl chains to the C-2 position of CO, we designed and synthesized a series of novel CO amide derivatives 8a–l (Figure 1) to improve their water solubility and antiproliferative activities. Meanwhile, their preliminary antitumor activity mechanism was further investigated.

2. RESULTS AND DISCUSSION

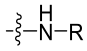
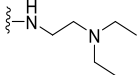
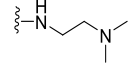
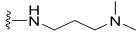
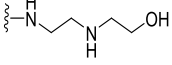
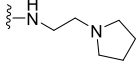
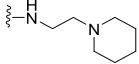
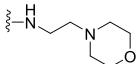
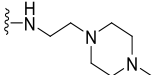
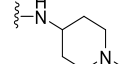
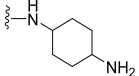
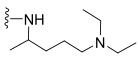
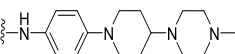
2.1. Synthesis. The synthetic route to compounds 8a–l is described in Scheme 1. L-Tryptophan methyl ester hydrochloride 1 was first reacted with dimethoxyacetaldehyde 2 via a Pictet-Spengler reaction to obtain intermediate 3, which was oxidized with KMnO_4 in THF to afford compound 4. Then, compound 4 was hydrolyzed with acetic acid to provide intermediate 5. Acetic anhydride and sodium carbonate were reacted with intermediate 5 to carry out the cyclization reactions of 5 and form the key intermediate 6. Finally, intermediate 6 was treated with different substituted primary amines 8a–l in methanol to produce the target compounds

8a–l with >95% purity, and the structures of these compounds were characterized through MS, $^1\text{H}/^{13}\text{C}$ NMR, and HRMS (the detailed original characterization spectrograms are listed in the Supporting Information).

Generally, CO is obtained through cyclization and decarboxylation reaction using both *N*-benzyltryptamine and α -ketoglutaric acid as the raw materials. However, such a synthetic route almost takes 60 h, and the post-treatment is complex; also, the yield is low (35–55%).^{24,25} In this paper, we use L-tryptophan methyl ester hydrochloride as the raw material to obtain the target compound, through the Pictet-Spengler cyclization condensation reaction, oxidation, hydrolysis, and condensation cyclization, which not only have the advantages of short reaction time and a simple post-treatment method but also can further modify to obtain CO derivatives.

2.2. Antiproliferative Activity. Using four human cancer cell lines, the antiproliferative effects of target compounds 8a–l were evaluated through the thiazolyl blue tetrazolium bromide (MTT) assay. CO was also tested for comparison. The four human cancer cell lines included colon cancer cells (HT29),

Table 1. Cytotoxicity of Compounds 8a–l against Human HT29, H1975, A549, and MCF-7 Cancer Cells

Compounds		IC ₅₀ (μM) ^a			
		HT29	H1975	A549	MCF-7
CO	/	8.6 ± 0.7	10.7 ± 1.2	7.6 ± 0.6	8.9 ± 0.9
ADM	/	2.6 ± 0.4	ND ^b	3.0 ± 0.4	ND
8a		2.2 ± 0.3	ND	3.8 ± 0.5	4.7 ± 0.4
8b		2.9 ± 0.4	7.5 ± 0.6	3.2 ± 0.2	3.8 ± 0.3
8c		4.1 ± 0.3	7.7 ± 0.8	4.8 ± 0.4	4.6 ± 0.5
8d		2.6 ± 0.2	ND	4.2 ± 0.3	ND
8e		ND	ND	2.1 ± 0.3	4.5 ± 0.6
8f		1.7 ± 0.3	1.6 ± 0.1	2.0 ± 0.1	2.4 ± 0.2
8g		1.1 ± 0.1	1.3 ± 0.2	2.3 ± 0.1	2.9 ± 0.3
8h		1.0 ± 0.1	1.9 ± 0.3	1.3 ± 0.1	1.7 ± 0.2
8i		2.3 ± 0.3	3.0 ± 0.4	3.4 ± 0.3	4.6 ± 0.5
8j		ND	ND	3.5 ± 0.4	5.9 ± 0.5
8k		4.3 ± 0.5	5.5 ± 0.7	ND	3.8 ± 0.3
8l		>10	>10	>10	>10

^aCytotoxicity of tested compound incubated for 72 h, and IC₅₀ data are expressed as mean ± s.d., *n* = 3. ^bNot detected.

lung adenocarcinoma cells (H1975), lung cancer cells (A549), breast cancer cells (MCF-7), and human normal colon epithelial cells (CCD841). Table 1 demonstrates that most target compounds 8a–l exhibited higher antiproliferative activity against the four cancer cells than the control CO, with their IC₅₀ values being in the single-digit micromolar range. Among the four cancer cells, 8a–l exhibited the strongest cytotoxicity against HT29 cells, with all IC₅₀ values lower than 5 μM. Therefore, HT29 cells were selected for further *in vitro* cell experiments. Most importantly, among all CO derivatives, 8h exhibited the lowest IC₅₀ of 1.0–1.9 μM against the four cancer cell lines, which was approximately 5–9-folds higher than that of CO (IC₅₀ = 7.6–10.7 μM). Interestingly, when the normal cell line CCD841 was incubated with 8h, there was 17-fold less cytotoxicity in CCD841 (IC₅₀ = 17.1 ± 2.5 μM) than that in HT29 cells

(IC₅₀ = 1.0 ± 0.1 μM). These results suggested that 8h possessed prominent cancer cell selective inhibitory effects.

2.3. Water Solubility of CO Derivatives. As shown in Table 2, we investigated whether the introduction of various nitrogen-containing heterocycles or alkyl chains to CO favored water solubility. The log_P value and water solubility of active

Table 2. Log_P and Solubility Value of CO and Its Derivatives

Compd	log _P	Solubility (μg/mL)
CO	1.87	16.1 ± 1.0
8f	2.17	41.3 ± 4.5
8g	1.03	92.9 ± 4.8
8h	1.19	70.5 ± 3.6
8i	1.38	60.4 ± 5.4

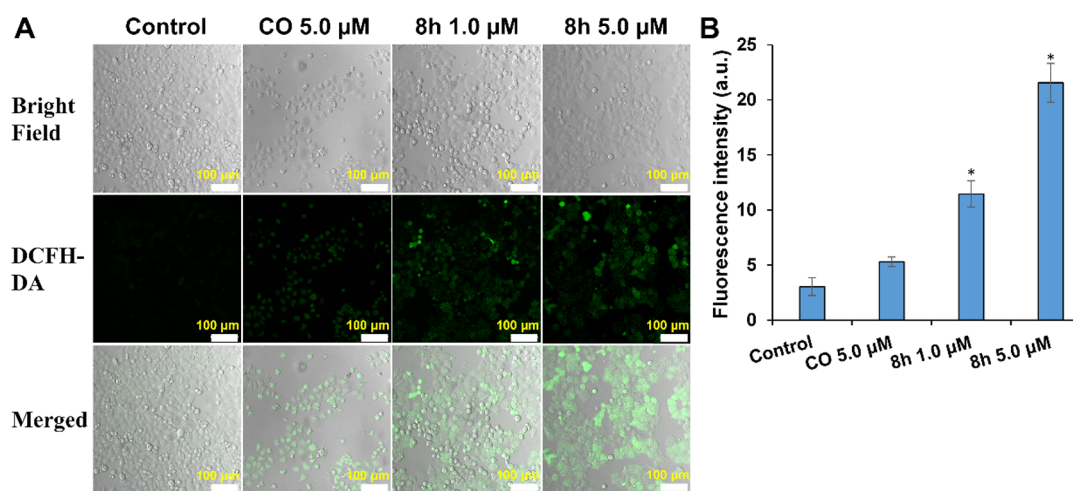


Figure 2. Compound **8h** induced ROS accumulation after 12 h treatment. (A) ROS measurement in HT29 cells under different treatments using the DCFH-DA probe. Scale bars: 100 μm . (B) Fluorescence intensity of HT29 cells after different treatments. The related data are presented as the means \pm SD of three separate assays. * $P < 0.01$ vs control.

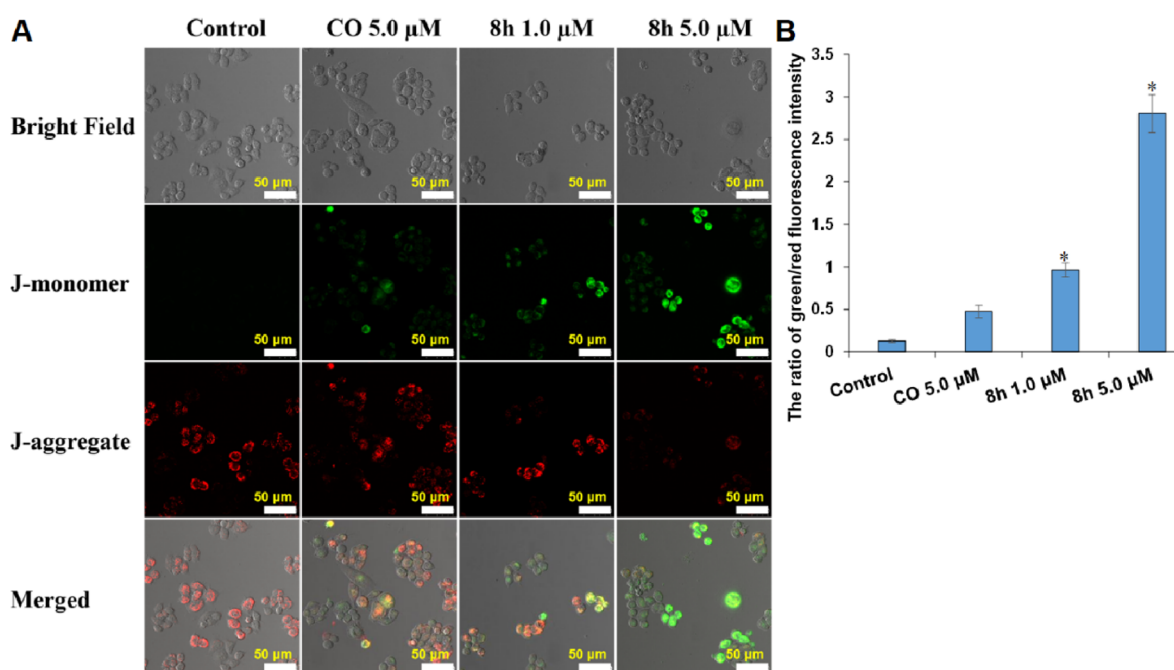


Figure 3. Compound **8h** induced MMP loss in HT29 cells. (A) MMP of HT29 cells under different treatments was measured with JC-1 dye. Scale bar = 50 μm . The photographs were taken with a confocal laser-scanning microscope (CLSM). (B) Ratio of green/red fluorescence intensity. The related data are presented as the means \pm SD of three separate assays. * $P < 0.01$ vs control.

CO derivatives **8f–i** was evaluated using the UV method, adapted from known protocols.²⁶ Improved water solubility was observed compared with CO. Notably, the water solubility of compound **8g** was the highest (up to $92.9 \pm 4.8 \mu\text{g/mL}$) with the lowest $\log P$ and was nearly 6-fold higher than that of CO. These results suggested that substitution of the nitrogen-containing group at the C-2 position contributed to the improvement in water solubility.

2.4. Structure–Activity Relationships. As discussed earlier, compounds **8a–m** with the hydrophilic nitrogen group at the C-2 position exhibited higher cytotoxic potencies than CO against the four human cancer cell lines. By contrast, the introduction of arylamine (e.g., **8l**) impaired its cytotoxic activity. Furthermore, the activities of compounds **8e–j** containing hydrophilic saturated nitrogen-containing hetero-

cycles were slightly higher than those of compounds **8a–d** and **8k** with hydrophilic nitrogen-containing alkyl fragments. **8e–j** exhibited a higher antiproliferative activity than **8a–d**, suggesting that the substitution of *N*-heterocyclic groups at the C-2 position was slightly superior to that of straight-chain alkanes or amino alcohols. Among **8e–j**, *N*-methylpiperazine-substituted compound **8h** was the most effective in this series, and its IC_{50} value ($1.0 \pm 0.1 \mu\text{M}$ against HT29 cells) was 8.6-fold lower than that of the control CO. The detailed structure–activity relationships will be further studied.

2.5. Compound 8h Increased Reactive Oxygen Species Levels in HT29 Cells. Increasing reactive oxygen species (ROS) levels have gradually become a promising antitumor strategy because of the vital role of ROS in redox signaling pathways.^{27–29} To verify whether the antiproliferative

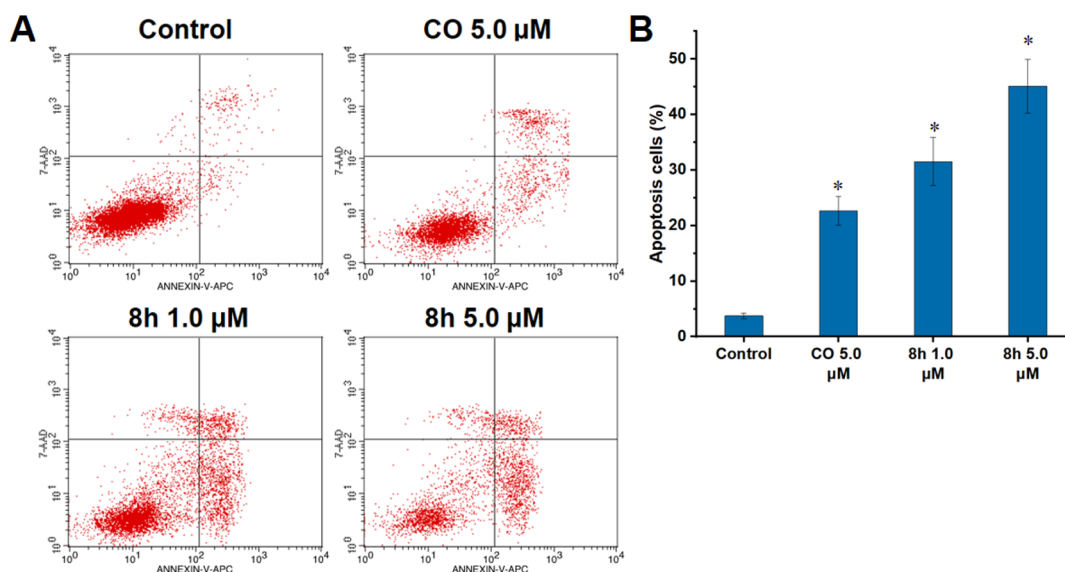


Figure 4. Compound **8h** induced HT29 cells apoptosis *in vitro*. (A) Flow cytometry analysis of HT29 cells under different treatments, after staining with FITC-annexin V/PI. (B) Quantitative analysis of early + late apoptotic cells. The related data are presented as the means \pm SD of three separate assays. * $P < 0.01$ vs control.

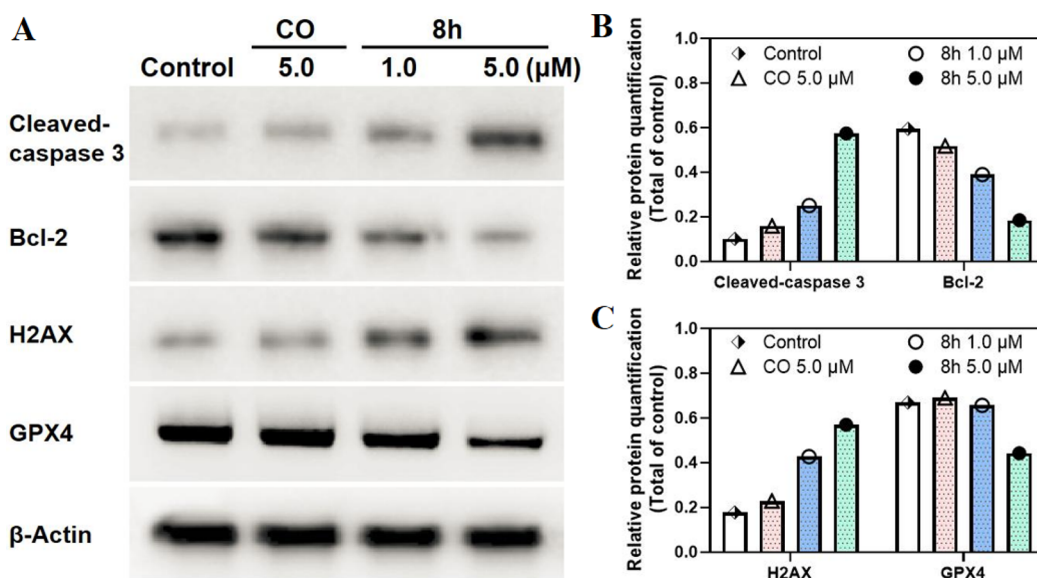


Figure 5. (A) Levels of cleaved-caspase 3, Bcl-2, H2AX, and GPX4 in HT29 cells under different treatments by Western blotting. (B, C) the relative protein quantitative analysis (cleaved-caspase 3, Bcl-2, H2AX, and GPX4) when compared with β -actin.

potency of compound **8h** is related to the increase in ROS levels, the ROS detection probe DCFH-DA was used to evaluate the effect of **8h** on intracellular ROS levels of HT29 cells. Almost no fluorescence signal was observed in the PBS group, and a weak fluorescence signal was detected in HT29 cells treated with CO at 5.0 μ M (Figure 2). Intense green fluorescence was observed in the **8h**-treated cells, and the fluorescence intensity was proportional to the **8h** concentration. Notably, **8h** exhibited a stronger capability to induce intracellular ROS accumulation at 1.0 or 5.0 μ M than CO. The results indicated that **8h** could increase the intracellular ROS level, induce oxidative stress, and thus produce significant cytotoxicity.

2.6. Compound 8h Decreased the Mitochondrial Membrane Potential (MMP) in HT29 Cells. An increase in the ROS level can lead to mitochondrial DNA damage,

reduce ATP production, and ultimately trigger a reduction in MMP.³⁰ Therefore, the MMP probe JC-1 was used to investigate the effect of compound **8h** on the MMP of HT29 cells. Under the normal MMP condition, JC-1 can form J-aggregates in the mitochondrial matrix and emit red fluorescence. However, this probe also exists as a monomer and emits green fluorescence when MMP is below normal levels.³¹ As depicted in Figure 3, a weaker red fluorescence signal and a significantly enhanced intensity of the green fluorescence signal were observed in the **8h** group compared with the CO group. Moreover, the intracellular red fluorescence almost disappeared when the **8h** concentration increased to 5 μ M. The fluorescence change from green to red reflected that **8h** could significantly induce mitochondrial damage.

2.7. Compound 8h-Induced Apoptosis of HT29 Cells.

Intracellular oxidative stress and mitochondrial damage can promote cell apoptosis.^{29,32} Therefore, we investigated the levels of 8h-induced apoptosis of HT29 cells. After CO (5.0 μM) or 8h (1.0 and 5.0 μM) treatment, HT29 cells were co-stained with annexin V-FITC and propidium iodide (PI), and the levels of apoptotic cells were analyzed through flow cytometry. In Figure 4, the percentage of apoptotic cells including early and late apoptotic cells in the 8h-treated group increased in a concentration-dependent manner (31.55% for 1.0 μM and 45.14% for 5.0 μM), which was significantly higher than that in the group of HT29 cells treated with 5.0 μM CO (22.68%). This indicated that 8h could effectively induce cell apoptosis.

Caspase 3 and Bcl-2 as apoptosis proteins play crucial roles in regulating apoptosis.³³ To verify the capability of 8h to induce apoptosis, Bcl-2, and cleaved-caspase 3 expressions in 8h-treated HT29 cells were analyzed through Western blotting. As depicted in Figure 5, 8h remarkably led to cleavage of caspase-3 and reduced the expression of antiapoptotic Bcl-2 protein in a dose-dependent manner (1.0 and 5.0 μM); these effects were more potent than those of CO treatment in HT29 cells. Together, these experimental results further confirmed the apoptosis-inducing efficacy of 8h.

2.8. Compound 8h-Induced DNA Damage in HT29

Cells. The antiproliferative activity of CO may be related to its induction of DNA damage.^{23,34} Therefore, the expression of H2AX, a biomarker of DNA damage, in HT29 cells was evaluated through Western blotting to investigate whether the CO derivative 8h could induce DNA damage. Figure 5 demonstrates that CO (5.0 μM) could increase H2AX expression to a certain extent (approximately 1.3-fold). By contrast, 8h could increase H2AX expression in HT29 cells by 2.4-fold even at a small dose (1.0 μM) and by 3.2-fold at 5 μM , indicating that compound 8h was involved in inducing DNA damage.

2.9. Compound 8h-Induced Ferroptosis in HT29

Cells. Ferroptosis is a programmed cell death caused by the accumulation of lethal lipid peroxides.^{35–37} GSH is the main antioxidant in cells and the preferred GPX4 substrate. Therefore, the insufficient supply of GSH directly affects GPX4 function, resulting in ferroptosis.^{36,37} Regarding biochemical characteristics, ferroptosis is characterized by GSH depletion, GPX4 inactivation, and lipid peroxide accumulation. To further explore the relationship between the cytotoxicity of compound 8h and the induction of ferroptosis, the levels of key ferroptosis-associated indicators (GSH, lipid peroxidation, and GPX4) were detected. As shown in Figures 5 and 6, compared with CO, 8h markedly reduced both the GSH level and GPX4 expression in a dose-dependent manner and increased the level of malondialdehyde (MDA), which is an important parameter of lipid peroxidation and positive-regulation on ferroptosis. These results indicated that the antiproliferative activity of 8h was also related to its induction of ferroptosis.

3. CONCLUSIONS

In summary, a series of novel CO derivatives (8a–1) containing the nitrogen-containing group at the C-2 position were designed and synthesized, and their *in vitro* antitumor activity and a series of preliminary mechanisms were investigated. The majority of compounds displayed antiproliferative potencies against four human cancer cell lines,

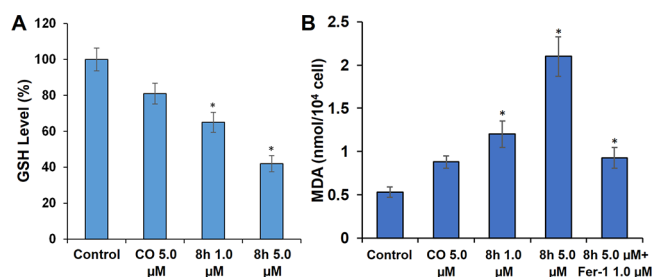


Figure 6. Compound 8h reduced the level of GSH and lipid peroxidation in HT29 cells. (A) Quantitative analysis of GSH levels. HT29 cells were applied with different concentrations of CO or compound 8h for 24 h. (B) Quantitative analysis of lipid peroxidation levels were applied with compound 8h (5 μM) or ferrostatin-1 (Fer-1, 1 μM). Means \pm SD, $n = 3$, * $p < 0.01$.

especially HT29 cells, at single-digit micromolar concentrations. As the most potent *N*-heterocyclic-substituted CO derivative, 8h exhibited 5–9-fold higher cytotoxicity than CO against the four cancer cells. Notably, 8h increased the intracellular ROS level and induced mitochondrial damage more potently than CO. Flow cytometry and Western blotting demonstrated the excellent ability of 8h to induce apoptosis and DNA damage in the HT29 cells. Moreover, the up-regulation of lipid peroxidation levels and the down-regulation of both the GSH level and GPX4 expression revealed that the induction of ferroptosis was another crucial mechanism for the antiproliferative activity of 8h. These results suggested that the novel CO derivative 8h with *N*-methylpiperazine substitution may be a promising candidate in the development of novel anti-colon cancer drugs.

4. EXPERIMENTAL SECTIONS

4.1. Materials and Reagents. All chemicals and solvents were purchased from commercial suppliers and used without further purification. All reactions were monitored by tetramethylsilane (TLC). Reaction products were purified by column chromatography on silica gel (200–300 mesh). ¹H and ¹³C NMR spectra were obtained in DMSO-*d*₆ or CDCl₃ solvents, with TMS as the internal standard. The purities of target compounds were over 95%, as determined by HPLC. High-resolution mass spectra (HRMS) data were collected on a JMS-SX102A (FAB) or LC/MSD TOF. UV–vis absorption spectra were measured on a spectrometer (UV1800PC, Jinghua, China). The synthesis process of compounds 3–6 were referred to the previous articles.^{38–40}

4.2. Synthesis of 8a–1. **4.2.1. *N*-(2-(Diethylamino)ethyl)-6-oxo-6H-indolo[3,2,1-de][1,5]naphthyridine-2-carboxamide (8a).** A solution of compound 6 (200 mg, 0.7187 mmol) was dissolved in 4 mL of methanol and then added *N*¹,*N*¹-diethyl-1,2-ethylamine (835.20 mg, 7.187 mmol). The reaction was stirred at 80 °C for 12 h. After completion, the mixture was extracted with dichloromethane and the organic phase was concentrated and purified by column chromatography (MeOH: DCM = 1:50) to afford faint yellow solid compound 8a (78%). ¹H NMR (400 MHz, DMSO-*d*₆) δ 9.01 (s, 1H, NH), 8.16 (m, 1H, Ar–H), 8.00 (d, $J = 8.1$ Hz, 1H, Ar–H), 7.72 (m, 1H, Ar–H), 7.64 (d, $J = 9.8$ Hz, 1H, =CH), 7.42 (m, 1H, Ar–H), 7.27 (m, 1H, Ar–H), 6.62 (d, $J = 9.8$ Hz, 1H, =CH), 3.50 (m, 2H, CH₂), 2.75 (m, 2H, CH₂), 2.68 (m, 4H, 2CH₂), 1.11 (m, 6H, 2CH₃). ¹³C NMR (101 MHz, DMSO-*d*₆) δ 164.4, 158.7, 145.9, 138.6, 133.6, 131.9, 130.5, 130.0,

128.8, 125.5, 123.5, 122.5, 116.0, 114.4, 51.2, 48.2, 47.1, 10.3. HRMS (ESI): m/z calcd for $C_{21}H_{22}N_4O_2$: 363.1816, found, 363.1825 $[M + H]^+$.

4.2.2. *N*-(2-(Dimethylamino)ethyl)-6-oxo-6H-indolo[3,2,1-de][1,5]naphthyridine-2-carboxamide (8b). According to the synthesis method of compound **8a**, N^1,N^1 -diethyl-1,2-ethylamine was replaced with N^1,N^1 -dimethyl-1,2-ethylamine to obtain faint yellow solid compound **8b** (70%). 1H NMR (DMSO- d_6 , 400 MHz) δ 9.40 (s, 1H, NH), 8.75 (m, 1H, Ar-H), 8.39–8.47 (m, 1H, Ar-H), 8.16 (d, H, $J = 9.8$ Hz, =CH), 7.68 (m, 1H, Ar-H), 7.59 (m, 1H, Ar-H), 7.30 (m, 1H, Ar-H), 6.67 (d, H, $J = 9.8$ Hz, =CH), 3.89 (s, 3H, CH_3), 3.66 (m, 2H, CH_2), 2.72 (m, 2H, CH_2). ^{13}C NMR (101 MHz, DMSO- d_6) δ 164.0, 159.4, 147.2, 139.7, 133.3, 131.5, 131.1, 130.3, 126.3, 124.8, 124.7, 124.5, 116.8, 116.3, 56.4, 45.7, 40.0. HRMS (ESI): m/z calcd for $C_{19}H_{18}N_4O_2$: 335.1503, found, 335.1502 $[M + H]^+$.

4.2.3. *N*-(3-(Dimethylamino)propyl)-6-oxo-6H-indolo[3,2,1-de][1,5]naphthyridine-2-carboxamide (8c). According to the synthesis method of compound **8a**, N^1,N^1 -diethyl-1,2-ethylamine was replaced with N^1,N^1 -dimethylpropane-1,3-diamine to obtain faint yellow solid compound **8c** (65%). 1H NMR (400 MHz, DMSO- d_6) δ 9.10 (m, 1H, NH), 8.93 (s, 1H, Ar-H), 8.48 (dd, $J = 12.6, 8.0$ Hz, 2H, 2Ar-H), 8.10 (d, $J = 9.8$ Hz, 1H, =CH), 7.76 (m, 1H, Ar-H), 7.59 (m, 1H, Ar-H), 7.05 (d, $J = 9.8$ Hz, 1H, Ar-H), 3.45–3.40 (m, 2H, CH_2), 2.36 (m, 2H, CH_2), 2.21 (s, 6H, 2 CH_3), 1.79–1.69 (m, 2H, CH_2). ^{13}C NMR (101 MHz, DMSO- d_6) δ 164.0, 159.3, 147.4, 139.7, 139.6, 139.5, 134.4, 134.4, 133.1, 133.1, 131.5, 130.9, 130.9, 130.0, 126.3, 124.6, 124.6, 124.5, 116.6, 116.2, 65.4, 57.7, 56.5, 45.6, 40.1, 39.9, 39.7, 39.5, 39.3, 38.4, 31.7, 29.4, 29.0, 27.3, 27.0, 22.5, 19.0, 14.3. HRMS (ESI): m/z calcd for $C_{20}H_{20}N_4O_2$: 349.1586, found, 349.1649 $[M + H]^+$.

4.2.4. *N*-(2-((2-Hydroxyethyl)amino)ethyl)-6-oxo-6H-indolo[3,2,1-de][1,5]naphthyridine-2-carboxamide (8d). According to the synthesis method of compound **8a**, N^1,N^1 -diethyl-1,2-ethylamine was replaced with 2-(2-aminoethyl)ethyl alcohol to obtain faint yellow solid compound **8d** (48%). 1H NMR (400 MHz, DMSO- d_6) δ 9.03 (s, 1H, Ar-H), 8.86 (m, 1H, CONH), 8.56 (dd, $J = 14.4, 7.9$ Hz, 2H, Ar-H), 8.18 (d, $J = 9.8$ Hz, 1H, CH_2), 7.82 (m, 1H, Ar-H), 7.64 (m, 1H, Ar-H), 7.10 (d, $J = 9.8$ Hz, 1H, CH_2), 2.95 (s, 1H, OH), 2.78 (m, 2H, CH_2), 2.64 (m, 2H, CH_2), 2.61 (m, 2H, CH_2), 2.44 (m, 2H, CH_2). ^{13}C NMR (101 MHz, DMSO- d_6) δ 164.0, 159.4, 147.2, 140.0, 139.7, 134.6, 133.3, 131.7, 131.5, 131.1, 130.3, 130.0, 126.3, 124.8, 124.7, 124.5, 116.8, 116.5, 116.3, 58.5, 56.4, 55.3, 45.7, 45.5, 37.4, 19.1, 18.8. HRMS (ESI): m/z calcd for $C_{19}H_{18}N_4O_3$: 351.1452, found: 351.1457 $[M + H]^+$.

4.2.5. 6-Oxo-*N*-(2-(pyrrolidin-1-yl)ethyl)-6H-indolo[3,2,1-de][1,5]naphthyridine-2-carboxamide (8e). According to the synthesis method of compound **8a**, N^1,N^1 -diethyl-1,2-ethylamine was replaced with 2-(pyrrolidine-1-yl)ethylamine to obtain faint yellow solid compound **8e** (62%). 1H NMR (400 MHz, DMSO- d_6) δ 9.00 (s, 1H, NH), 8.81 (m, 1H, Ar-H), 8.53 (d, $J = 8.0$ Hz, 2H, Ar-H), 8.15 (d, $J = 9.8$ Hz, 1H, CH=), 7.80 (m, 1H, Ar-H), 7.62 (m, 1H, Ar-H), 7.08 (d, $J = 9.8$ Hz, 1H, CH=), 3.52 (m, 2H, CH_2), 2.67 (m, 2H, CH_2), 2.52 (m, 4H, 2 CH_2), 1.71 (m, 4H, 2 CH_2). ^{13}C NMR (101 Hz, DMSO- d_6) δ 164.1, 159.5, 147.2, 139.9, 139.6, 134.5, 133.3, 131.1, 130.3, 130.0, 126.4, 124.8, 124.7, 116.9, 116.3, 56.4, 55.2, 54.0, 23.6. HRMS (ESI): m/z calcd for $C_{21}H_{20}N_4O_2$: 361.1659, found: 361.1652 $[M + H]^+$.

4.2.6. 6-Oxo-*N*-(2-(piperidin-1-yl)ethyl)-6H-indolo[3,2,1-de][1,5]naphthyridine-2-carboxamide (8f). According to the synthesis method of compound **8a**, N^1,N^1 -diethyl-1,2-ethylamine was replaced with 2-piperidinethylamine to obtain white solid compound **8f** (66%). 1H NMR (400 MHz, DMSO- d_6) δ 8.79 (s, 1H, NH), 8.52 (d, $J = 8.2$ Hz, 1H, Ar-H), 8.20 (d, $J = 7.8$ Hz, 1H, Ar-H), 8.12 (d, $J = 8.2$ Hz, 1H, Ar-H), 8.04 (d, $J = 9.8$ Hz, 1H, =CH), 7.70 (m, 1H, Ar-H), 7.54 (m, 1H, Ar-H), 6.99 (d, $J = 9.8$ Hz, 1H, =CH), 3.71–3.74 (m, 4H, 2 CH_2), 3.63 (m, 2H, CH_2), 3.27 (t, $J = 1.5$ Hz, 2H, CH_2), 2.66 (m, 2H, CH_2), 2.56 (m, 4H, 2 CH_2). ^{13}C NMR (101 MHz, DMSO- d_6) δ 164.7, 159.5, 146.2, 139.5, 134.3, 132.9, 131.0, 130.8, 129.1, 125.8, 124.2, 116.4, 115.0, 57.5, 54.1, 48.1, 25.1, 23.6. HRMS (ESI): m/z calcd for $C_{22}H_{22}N_4O_2$: 375.1816, found, 375.1809 $[M + H]^+$.

4.2.7. *N*-(2-(Morpholino)ethyl)-6-oxo-indole [3,2,1-de]-[1,5]naphthyridin-2-formamide (8g). According to the synthesis method of compound **8a**, N^1,N^1 -diethyl-1,2-ethylamine was replaced with 2-morpholine ethylamine to obtain pink solid compound **8g** (73%). 1H NMR (400 MHz, DMSO- d_6) δ 9.40 (s, 1H, NH), 8.79 (s, 1H, Ar-H), 8.52 (d, $J = 8.2$ Hz, 1H, Ar-H), 8.20 (d, $J = 7.8$ Hz, 1H, Ar-H), 8.04 (d, $J = 9.8$ Hz, 1H, =CH), 7.70 (m, Ar-H), 7.54 (m, 1H, Ar-H), 6.99 (d, $J = 9.8$ Hz, 1H, =CH), 3.74–3.71 (m, 4H, 2 CH_2), 3.63 (m, 2H, CH_2), 3.27 (d, $J = 1.5$ Hz, 2H, CH_2), 2.66 (m, 2H, CH_2), 2.56 (m, 4H, 2 CH_2). ^{13}C NMR (101 MHz, DMSO- d_6) δ 164.7, 159.6, 146.4, 139.6, 134.3, 133.3, 131.4, 131.1, 129.3, 126.0, 124.3, 123.0, 116.8, 115.4, 77.4, 66.6, 53.3, 48.8. HRMS (ESI): m/z calcd for $C_{21}H_{20}N_4O_3$: 377.1608, found, 377.1613 $[M + H]^+$.

4.2.8. *N*-(2-(4-Methylpiperazin-1-yl)ethyl)-6-oxo-6H-indolo[3,2,1-de][1,5]naphthyridine-2-carboxamide (8h). According to the synthesis method of compound **8a**, N^1,N^1 -diethyl-1,2-ethylamine was replaced with 2-piperazineethylamine to obtain faint yellow solid compound **8h** (60%). 1H NMR (400 MHz, DMSO- d_6) δ 8.77 (s, 1H, NH), 8.49 (d, $J = 8.2$ Hz, 2H, 2Ar-H), 8.24 (d, $J = 7.5$ Hz, 1H, Ar-H), 8.05 (d, $J = 9.8$ Hz, 1H, =CH), 7.71 (m, 1H, Ar-H), 7.55 (m, 1H, Ar-H), 6.98 (d, $J = 9.8$ Hz, 1H, =CH), 3.63 (m, 2H, CH_2), 3.28 (m, 6H, 3 CH_2), 2.65 (m, 2H, CH_2), 2.56 (m, 4H, 2 CH_2). ^{13}C NMR (101 MHz, DMSO- d_6) δ 161.3, 159.4, 151.1, 141.2, 139.5, 135.8, 130.4, 129.7, 126.8, 124.3, 124.1, 121.4, 119.5, 115.2, 105.2, 57.3, 53.2, 46.6. HRMS (ESI): m/z calcd for $C_{22}H_{23}N_5O_2$: 390.1925, found, 390.1929 $[M + H]^+$.

4.2.9. *N*-(1-Methylpiperidin-4-yl)-6-oxo-6H-indolo[3,2,1-de][1,5]naphthyridine-2-carboxamide (8i). According to the synthesis method of compound **8a**, N^1,N^1 -diethyl-1,2-ethylamine was replaced with 1-methylpiperidine-4-amine to obtain faint yellow solid compound **8i** (65%). 1H NMR (400 MHz, DMSO- d_6) δ 8.96 (s, 1H, NH), 8.60 (d, $J = 8.1$ Hz, 1H, Ar-H), 8.51 (d, $J = 7.5$ Hz, 2H, 2Ar-H), 8.18 (d, $J = 9.8$ Hz, 1H, =CH), 7.78 (m, 1H, Ar-H), 7.61 (m, 1H, Ar-H), 7.07 (d, $J = 9.8$ Hz, 1H, =CH), 3.85 (m, 1H, CH), 2.78 (d, $J = 11.1$ Hz, 4H, 2 CH_2), 2.51 (s, 3H, CH_3), 2.01 (m, 2H, CH_2), 1.73 (d, $J = 20.7, 11.4$ Hz, 2H, CH_2). ^{13}C NMR (101 MHz, DMSO- d_6) δ 163.5, 159.4, 147.2, 139.9, 134.5, 133.2, 131.7, 131.5, 130.2, 129.9, 126.3, 124.7, 124.6, 116.5, 116.4, 54.5, 46.7, 46.3, 31.4. HRMS (ESI): m/z calcd for $C_{21}H_{20}N_4O_2$: 361.1659, found, 361.1656 $[M + H]^+$.

4.2.10. *N*-(4-Aminocyclohexyl)-6-oxo-6H-indolo[3,2,1-de]-[1,5]naphthyridine-2-carboxamide (8j). According to the synthesis method of compound **8a**, N^1,N^1 -diethyl-1,2-ethylamine was replaced with cyclohexane-1,4-diamine to obtain

faint yellow solid compound **8j** (68%). ^1H NMR (400 MHz, DMSO- d_6) δ 8.94 (s, 1H, NH), 8.39–8.56 (m, 3H, Ar–H), 8.15 (d, $J = 9.8$ Hz, 1H, =CH), 7.78 (d, $J = 7.7$ Hz, 1H), 7.60 (d, $J = 7.6$ Hz, 1H), 7.06 (d, $J = 9.8$ Hz, 1H, =CH), 3.82 (m, 1H, –NHCH), 2.59 (m, 1H, –NH $_2$ CH), 1.85 (m, 4H, CH $_2$), 1.18 (m, 4H, CH $_2$). ^{13}C NMR (101 MHz, DMSO- d_6) δ 163.3, 159.3, 147.2, 139.8, 139.6, 134.5, 133.3, 131.6, 130.1, 126.4, 124.8, 124.6, 116.9, 116.3, 50.1, 48.5, 35.4, 31.5. HRMS (ESI): m/z calcd for $\text{C}_{21}\text{H}_{20}\text{N}_4\text{O}_2$: 361.1659, found: 361.1662 [$\text{M} + \text{H}$] $^+$.

4.2.11. *N*-(5-(Diethylamino)pentan-2-yl)-6-oxo-6H-indolo[3,2,1-de][1,5]naphthyridine-2-carboxamide (8k). According to the synthesis method of compound **8a**, N^1, N^1 -diethyl-1,2-ethylamine was replaced with N^1, N^1 -diethylpentane-1,4-diamine to obtain faint yellow solid compound **8k** (51%). ^1H NMR (400 MHz, DMSO- d_6) δ 9.01 (s, 1H, Ar–H), 8.54 (dd, $J = 12.8, 7.3$ Hz, 1H, Ar–H), 8.19 (s, 1H, CONH), 7.80 (m, 1H, Ar–H), 7.63 (m, 1H, CH $_2$), 7.09 (d, $J = 9.8$ Hz, 1H, CH $_2$), 4.14 (m, 1H, CH), 2.49–2.34 (m, 6H, CH $_2$), 1.68–1.53 (m, 2H, CH $_2$), 1.46 (t, $J = 6.6$ Hz, 2H, CH $_2$), 1.23 (s, 3H, CH $_3$), 0.93 (m, 6H, 2CH $_3$). ^{13}C NMR (101 MHz, DMSO- d_6) δ 163.5, 159.4, 147.5, 139.8, 139.7, 134.5, 133.2, 131.6, 131.1, 130.1, 126.3, 124.7, 124.6, 116.7, 116.4, 52.5, 46.7, 45.3, 34.3, 24.0, 21.3, 12.0. HRMS (ESI): m/z calcd for $\text{C}_{24}\text{H}_{28}\text{N}_4\text{O}_2$: 405.2291, found: 405.2291 [$\text{M} + \text{H}$] $^+$.

4.2.12. *N*-(4-(4-(4-Methylpiperazin-1-yl)piperidin-1-yl)phenyl)-6-oxo-6H-indolo[3,2,1-de][1,5]naphthyridine-2-carboxamide (8l). According to the synthesis method of compound **8a**, N^1, N^1 -diethyl-1,2-ethylamine was replaced with 4-(4-(4-methylpiperazin-1-yl)piperidin-1-yl)aniline to obtain faint yellow solid compound **8l** (60%). ^1H NMR (400 MHz) δ 8.94 (s, 1H, NH), 8.55–8.40 (m, 3H, 3Ar–H), 8.15 (d, $J = 9.8$ Hz, 1H, =CH), 7.78 (m, 1H, Ar–H), 7.60 (m, 1H, CH=CH), 7.35 (d, $J = 9.9$ Hz, 2H, 2Ar–H), 7.06 (d, $J = 9.8$ Hz, 1H, =CH), 6.56 (d, $J = 9.8$ Hz, 2H, 2Ar–H), 3.83 (m, 2H, CH $_2$), 2.26 (s, 3H, CH $_3$), 1.94–1.79 (m, 4H, 2CH $_2$), 1.52 (m, 2H, CH $_2$), 1.33–1.04 (m, 4H, 2CH $_2$), 0.87–0.80 (m, 4H, 2CH $_2$). ^{13}C NMR (101 MHz, DMSO- d_6) δ 157.0, 156.8, 156.4, 151.6, 151.3, 150.8, 150.6, 150.3, 138.2, 129.4, 129.1, 128.3, 127.8, 125.7, 124.8, 124.4, 119.3, 115.8, 60.6, 53.2, 48.5, 21.1. HRMS (ESI): m/z calcd for $\text{C}_{31}\text{H}_{32}\text{N}_6\text{O}_2$: 521.2587, found: 521.2553 [$\text{M} + \text{H}$] $^+$.

4.3. Cell Culture. Colon cancer cell line (HT29), lung adenocarcinoma cells line (H1975), lung cancer cell line (A549), breast cancer cell line (MCF 7), and human normal colon epithelial cells (CCD841) were routinely cultured in DMEM/RPMI 1640 complete culture medium into a CO_2 incubator where the percentage of CO_2 is 5% and incubated temperature is 37 °C.

4.4. MTT Assay. Cytotoxicity was determined using an MTT experiment.⁴¹ The cancer and normal cells were cultured in 96-well plates (5×10^5 cells/mL) for 24 h. The groups were incubated with different concentration of CO or **8a–I** (0.5, 1.0, 2.0, 5.0, or 12.5 μM) in 100 μL of DMEM culture medium for 24 h and then cultured for another 72 h. The medium was removed, and 10 μL of 5 mg/mL MTT solution was added to each plate; the cells were then incubated at 37 °C for 4 h. This medium was removed, and the formazan crystals were dissolved in 100 μL DMSO. A multifunctional microplate reader (Synergy H1, Bio-Tek, USA) was used to record the absorbance of the solution in each well at 490 nm.

4.5. Water Solubility of CO Derivatives. The log P value and water solubility of active CO derivatives **8a–I** was

evaluated using the UV method. CO or compound **8a–I** were mixed into five concentrations in methanol/water (V:V = 1:1), respectively. The UV spectrophotometer was used to measure the absorption of solutions with different concentrations, and the standard curve of each compound was obtained. Excessive compounds CO or compound **8a–I** was added in water to obtain saturated solutions after stewing for 2 h and filtered with filter membrane to measure the absorption of the solution, then substituted into the standard curve to obtain the concentration of the solution, and converted into water solubility.

4.6. Intracellular ROS Levels Detection. HT29 cells (approximately 1×10^4 cells per well) were incubated with CO (5.0 μM) or **8h** (1.0 or 5.0 μM) for 12 h. DCFH-DA (10 μM) was added for detecting reactive oxygen species, and the cells were incubated for 30 min. Finally, confocal microscope was used to obtain fluorescence image and green fluorescence of DCF ($\lambda_{\text{ex}} = 488$ nm, $\lambda_{\text{em}} = 500$ –550 nm).⁴²

4.7. Detection of MMP in HT29 Cells. The HT29 cells were cultured in 5% CO_2 at 37 °C for 24 h. Then, CO (5.0 μM) or **8h** (1.0 and 5.0 μM) were added per well and incubation was prolonged at 37 °C for 4 h. After incubation, the cells were incubated with JC-1 solution (10 $\mu\text{g}/\text{mL}$) at 37 °C for 20 min; afterward, the cells were washed with PBS for three times. Cell images were measured with a confocal fluorescence imaging system.⁴³ Green channel: Ex, 488 nm; Em, 510–545 nm; red channel: Ex, 535 nm; Em, 580–610 nm.

4.8. Apoptosis Assay. HT29 cells were seeded into a 6-well culture plate (2×10^4 cells/well) and incubated overnight. After incubation with CO (5.0 μM) or **8h** (1.0 and 5.0 μM) for 24 h. After another 72 h, the cells were harvested, washed in PBS, and stained with annexin V-FITC and propidium iodide (PI). The cell apoptosis was analyzed using the flow cytometer (FCM).⁴⁵

4.9. GSH and Lipid Peroxidation Level Assay. HT29 cells were treated with CO (5.0 μM) or **8h** (1.0 or 5.0 μM) to induce GSH depletion followed by harvesting to determine the cell number. We used the QuantiChrome glutathione assay kit and followed the product instructions to determine GSH levels.³⁵ HT29 cells were pretreated with or without ferrostatin-1 (1.0 μM) for 4 h and then treated with CO (5.0 μM) or **8h** (1.0 or 5.0 μM) to detect lipid peroxidation levels. Also, an MDA assay kit (S0131S, Shanghai Titan) was used to determine the levels of MDA.⁴⁶

4.10. Western Blot Analysis. HT29 cells were seeded in cell culture dish and cultured with medium containing CO (5.0 μM) or **8h** (1.0 or 5.0 μM), respectively. After 4 h of incubation, cells were lysed by RIPA lysis buffer with protease and phosphatase inhibitor in ice for 30 min. After measurement of protein concentration by the BCA assay, equal amounts of protein were added to each lane of SDS-PAGE gel for electrophoresis and then transferred onto polyvinylidene fluoride (PVDF) membranes. Antibodies for GPX4, Bcl-2, and cleaved-caspase 3 were used to detect their expression.^{44,47}

■ ASSOCIATED CONTENT

Supporting Information

The Supporting Information is available free of charge at <https://pubs.acs.org/doi/10.1021/acsomega.3c03358>.

^1H NMR, ^{13}C NMR, and HRMS spectra for **8a–I** and HPLC spectra for compounds **8h** (PDF)

AUTHOR INFORMATION

Corresponding Authors

Jinfeng Ding – Department of Pharmacy, Jiangsu Vocational College of Medicine, Yancheng 224005, China; School of Pharmacy and Jiangsu Province Key Laboratory for Inflammation and Molecular Drug Target, Nantong University, Nantong 226001, China; Email: dingjinfeng@jsmc.edu.cn

Yong Ling – School of Pharmacy and Jiangsu Province Key Laboratory for Inflammation and Molecular Drug Target and Nantong Key Laboratory of Small Molecular Drug Innovation, School of Pharmacy, Nantong University, Nantong 226001, China; orcid.org/0000-0002-3373-011X; Email: LYYY111@sina.com

Yanan Zhang – School of Pharmacy and Jiangsu Province Key Laboratory for Inflammation and Molecular Drug Target and Nantong Key Laboratory of Small Molecular Drug Innovation, School of Pharmacy, Nantong University, Nantong 226001, China; Email: yznj00@outlook.com

Authors

Tiantian Sun – School of Pharmacy and Jiangsu Province Key Laboratory for Inflammation and Molecular Drug Target and Nantong Key Laboratory of Small Molecular Drug Innovation, School of Pharmacy, Nantong University, Nantong 226001, China

Hongmei Wu – School of Pharmacy and Jiangsu Province Key Laboratory for Inflammation and Molecular Drug Target and Nantong Key Laboratory of Small Molecular Drug Innovation, School of Pharmacy, Nantong University, Nantong 226001, China

Hongwei Zheng – School of Pharmacy and Jiangsu Province Key Laboratory for Inflammation and Molecular Drug Target, Nantong University, Nantong 226001, China

Sijia Wang – School of Pharmacy and Jiangsu Province Key Laboratory for Inflammation and Molecular Drug Target and Nantong Key Laboratory of Small Molecular Drug Innovation, School of Pharmacy, Nantong University, Nantong 226001, China

Dezhi Wang – School of Pharmacy and Jiangsu Province Key Laboratory for Inflammation and Molecular Drug Target and Nantong Key Laboratory of Small Molecular Drug Innovation, School of Pharmacy, Nantong University, Nantong 226001, China

Wenpei Shan – School of Pharmacy and Jiangsu Province Key Laboratory for Inflammation and Molecular Drug Target, Nantong University, Nantong 226001, China

Complete contact information is available at:
<https://pubs.acs.org/10.1021/acsomega.3c03358>

Author Contributions

[†]J.D. and T.S. contributed equally.

Notes

The authors declare no competing financial interest.

ACKNOWLEDGMENTS

This work was supported by the National Natural Science Foundation of China (21977058), the Key Natural Science Foundation of Jiangsu Higher Education Institutions (20KJA350002), China Postdoctoral Science Foundation (2018T110533), the Natural Science Foundation of Nantong

City (MS12020047), and Jiangsu Province Innovation Project of Postgraduate Training (KYCX19 2086).

REFERENCES

- (1) Sung, H.; Ferlay, J.; Siegel, R. L.; Laversanne, M.; Soerjomataram, I.; Jemal, A.; Bray, F. Global cancer statistics 2020: GLOBOCAN estimates of incidence and mortality worldwide for 36 cancers in 185 countries. *CA-Cancer J. Clin.* **2021**, *71*, 209–249.
- (2) Chen, Q.; Ke, H.; Dai, Z.; Liu, Z. Nanoscale theranostics for physical stimulus-responsive cancer therapies. *Biomaterials* **2015**, *73*, 214–230.
- (3) Fan, J.-X.; Zheng, D.-W.; Mei, W.-W.; Chen, S.; Chen, S.-Y.; Cheng, S.-X.; Zhang, X.-Z. A metal-polyphenol network coated nanotheranostic system for metastatic tumor treatments. *Small* **2017**, *13*, 1702714.
- (4) Rayan, A.; Raiyn, J.; Falah, M. Nature is the best source of anticancer drugs: indexing natural products for their anticancer bioactivity. *PLoS One* **2017**, *12*, No. e0187925.
- (5) Guo, Z. The modification of natural products for medical use. *Acta Pharm. Sin. B* **2017**, *7*, 119–136.
- (6) Newman, D. J.; Cragg, G. M. Natural products as sources of new drugs from 1981 to 2014. *J. Nat. Prod.* **2016**, *79*, 629–661.
- (7) He, W.; Puyvelde, L. V.; Kimpe, N. D.; Verbruggen, L.; Anthonissen, K.; Flaas, M. V. d.; Bosselaers, J.; Mathenge, S. G.; Mudida, F. P. Chemical constituents and biological activities of *zanthoxylum usambarense*. *Phytother. Res.* **2002**, *16*, 66–70.
- (8) Devkota, K. P.; Wilson, J. A.; Henrich, C. J.; McMahon, J. B.; Reilly, K. M.; Beutler, J. A. Compounds from *simarouba berteroa* which inhibit proliferation of NF1-defective cancer cells. *Phytochem. Lett.* **2014**, *7*, 42–45.
- (9) Hsieh, P.-W.; Chang, F.-R.; Lee, K.-H.; Hwang, T.-L.; Chang, S.-M.; Wu, Y.-C. A new anti-HIV alkaloid, drymaritin, and a new *c*-glycoside flavonoid, diandraflavone, from *drymaria diandra*. *J. Nat. Prod.* **2004**, *67*, 1175–1177.
- (10) Bröckelmann, M. G.; Dasenbrock, J.; Steffan, B.; Steglich, W.; Wang, Y.; Raabe, G.; Fleischhauer, J. An unusual series of thiomethylated canthin-6-ones from the north american mushroom *boletus curtisii*. *Eur. J. Org. Chem.* **2004**, *2004*, 4856–4863.
- (11) Bharitkar, Y. P.; Hazra, A.; Apoorva Poduri, N. S.; Ash, A.; Maulik, P. R.; Mondal, N. B. Isolation, structural elucidation and cytotoxicity evaluation of a new pentahydroxy-pimarane diterpenoid along with other chemical constituents from *aerva lanata*. *Nat. Prod. Res.* **2015**, *29*, 253–261.
- (12) Lakshmi Manasa, K.; Thatikonda, S.; Sigalapalli, D. K.; Sagar, A.; Kiranmai, G.; Kalle, A. M.; Alvala, M.; Godugu, C.; Nagesh, N.; Nagendra Babu, B. Design and synthesis of β -carboline linked aryl sulfonyl piperazine derivatives: DNA topoisomerase II inhibition with DNA binding and apoptosis inducing ability. *Bioorg. Chem.* **2020**, *101*, No. 103983.
- (13) Peduto, A.; More, V.; de Caprariis, P.; Festa, M.; Capasso, A.; Piacente, S.; De Martino, L.; De Feo, V.; Filosa, R. Synthesis and cytotoxic activity of new β -carboline derivatives. *Mini-Rev. Med. Chem.* **2011**, *11*, 486–491.
- (14) Ammirante, M.; Di Giacomo, R.; De Martino, L.; Rosati, A.; Festa, M.; Gentilella, A.; Pascale, M. C.; Belisario, M. A.; Leone, A.; Caterina Turco, M.; De Feo, V. 1-Methoxy-canthin-6-one induces *c*-Jun NH2-terminal kinase-dependent apoptosis and synergizes with tumor necrosis factor-related apoptosis-inducing ligand activity in human neoplastic cells of hematopoietic or endodermal origin. *Cancer Res.* **2006**, *66*, 4385–4393.
- (15) O'Donnell, G.; Gibbons, S. Antibacterial activity of two canthin-6-one alkaloids from *allium neapolitanum*. *Phytother. Res.* **2007**, *21*, 653–657.
- (16) Ostrov, D. A.; Hernández Prada, J. A.; Corsino, P. E.; Finton, K. A.; Le, N.; Rowe, T. C. Discovery of novel DNA gyrase inhibitors by high-throughput virtual screening. *Antimicrob. Agents Chemother.* **2007**, *51*, 3688–3698.

- (17) Dejos, C.; Régnacq, M.; Bernard, M.; Voisin, P.; Bergès, T. The MFS-type efflux pump Flr1 induced by Yap1 promotes canthin-6-one resistance in yeast. *FEBS Lett.* **2013**, *587*, 3045–3051.
- (18) Ferreira, M. E.; Nakayama, H.; de Arias, A. R.; Schinini, A.; de Bilbao, N. V.; Serna, E.; Lagoutte, D.; Soriano-Agatón, F.; Poupon, E.; Hocquemiller, R.; Fournet, A. Effects of canthin-6-one alkaloids from *Zanthoxylum chiloperone* on *Trypanosoma cruzi*-infected mice. *J. Ethnopharmacol.* **2007**, *109*, 258–263.
- (19) Brahmabhatt, K. G.; Ahmed, N.; Sabde, S.; Mitra, D.; Singh, I. P.; Bhutani, K. K. Synthesis and evaluation of beta-carboline derivatives as inhibitors of human immunodeficiency virus. *Bioorg. Med. Chem. Lett.* **2010**, *20*, 4416–4419.
- (20) Guo, E.; Hu, Y.; Du, T.; Zhu, H.; Chen, L.; Qu, W.; Zhang, J.; Xie, N.; Liu, W.; Feng, F.; Xu, J. Effects of picrasma quassioides and its active constituents on alzheimer's disease in vitro and in vivo. *Bioorg. Chem.* **2019**, *92*, No. 103258.
- (21) Moss, G. P. Nomenclature of lignans and neolignans (IUPAC recommendations 2000). *Pure Appl. Chem.* **2000**, *72*, 1493–1523.
- (22) Dekebo, A.; Lang, M.; Polborn, K.; Dagne, E.; Steglich, W. Four lignans from commiphora erlangieriana. *J. Nat. Prod.* **2002**, *65*, 1252–1257.
- (23) Dejos, C.; Voisin, P.; Bernard, M.; Régnacq, M.; Bergès, T. Canthin-6-one displays antiproliferative activity and causes accumulation of cancer cells in the G2/M phase. *J. Nat. Prod.* **2014**, *77*, 2481–2487.
- (24) Dai, J.-K.; Dan, W.-J.; Li, N.; Du, H.-T.; Zhang, J.-W.; Wang, J.-R. Synthesis, in vitro antibacterial activities of a series of 3-N-substituted canthin-6-ones. *Bioorg. Med. Chem. Lett.* **2016**, *26*, 580–583.
- (25) Czerwinski, K. M.; Zifcsak, C. A.; Stevens, J.; Oberbeck, M.; Randlett, C.; King, M.; Mennen, S. An improved synthesis of Canthin-6-one. *Synth. Commun.* **2003**, *33*, 1225–1231.
- (26) Chen, T.-M.; Shen, H.; Zhu, C. Evaluation of a method for high throughput solubility determination using a multi-wavelength UV plate reader. *Comb. Chem. High Throughput Screen.* **2002**, *5*, 575–581.
- (27) Xian, D.; Lai, R.; Song, J.; Xiong, X.; Zhong, J. Emerging perspective: role of increased ROS and redox imbalance in skin carcinogenesis. *Oxid. Med. Cell. Longevity* **2019**, *2019*, 8127362.
- (28) Marengo, B.; Nitti, M.; Furfaro, A. L.; Colla, R.; Ciucis, C. D.; Marinari, U. M.; Pronzato, M. A.; Traverso, N.; Domenicotti, C. Redox homeostasis and cellular antioxidant systems: crucial players in cancer growth and therapy. *Oxid. Med. Cell Longevity* **2016**, *2016*, 6235641.
- (29) Wang, Y.; Liu, X.; Liu, G.; Wang, X.; Hu, R.; Liang, X. PIG11 over-expression predicts good prognosis and induces HepG2 cell apoptosis via reactive oxygen species-dependent mitochondrial pathway. *Biomed. Pharmacother.* **2018**, *108*, 435–442.
- (30) Wang, L.; Zheng, M.; Zhang, S.; Zhao, C.; Kang, W.; Wang, K. Roles of mtDNA damage and disordered Ca²⁺ homeostasis in the joint toxicities of cadmium and BDE209. *Ecotoxicol. Environ. Saf.* **2019**, *186*, No. 109767.
- (31) Malota, K.; Student, S.; Świątek, P. Low mitochondrial activity within developing earthworm male germ-line cysts revealed by JC-1. *Mitochondrion* **2019**, *44*, 111–121.
- (32) Xia, B.; Li, Q.; Zheng, K.; Wu, J.; Huang, C.; Liu, K.; You, Q.; Yuan, X. Down-regulation of Hrd1 protects against myocardial ischemia-reperfusion injury by regulating PPAR α to prevent oxidative stress, endoplasmic reticulum stress, and cellular apoptosis. *Eur. J. Pharmacol.* **2023**, *954*, No. 175864.
- (33) Mohamed, F. A. M.; Gomaa, H. A. M.; Hendawy, O. M.; Ali, A. T.; Farghaly, H. S.; Gouda, A. M.; Abdelazeem, A. H.; Abdelrahman, M. H.; Trembleau, L.; Youssif, B. G. M. Design, synthesis, and biological evaluation of novel EGFR inhibitors containing 5-chloro-3-hydroxymethyl-indole-2-carboxamide scaffold with apoptotic anti-proliferative activity. *Bioorg. Chem.* **2021**, *112*, No. 104960.
- (34) Vieira Torquato, H. F.; Ribeiro-Filho, A. C.; Buri, M. V.; Araújo Júnior, R. T.; Pimenta, R.; de Oliveira, J. S. R.; Filho, V. C.; Macho, A.; Paredes-Gamero, E. J.; de Oliveira Martins, D. T. Canthin-6-one induces cell death, cell cycle arrest and differentiation in human myeloid leukemia cells. *Biochim. Biophys. Acta, Gen. Subj.* **2017**, *1861*, 958–967.
- (35) Ursini, F.; Maiorino, M. Lipid peroxidation and ferroptosis: the role of GSH and GPx4. *Free Radicals Biol. Med.* **2020**, *152*, 175–185.
- (36) Wang, Y.; Zhang, Z.; Sun, W.; Zhang, J.; Xu, Q.; Zhou, X.; Mao, L. Ferroptosis in colorectal cancer: Potential mechanisms and effective therapeutic targets. *Biomed. Pharmacother.* **2022**, *153*, No. 113524.
- (37) Yang, W. S.; SriRamaratnam, R.; Welsch, M. E.; Shimada, K.; Skouta, R.; Viswanathan, V. S.; Cheah, J. H.; Clemons, P. A.; Shamji, A. F.; Clish, C. B.; Brown, L. M.; Girotti, A. W.; Cornish, V. W.; Schreiber, S. L.; Stockwell, B. R. Regulation of ferroptotic cancer cell death by GPX4. *Cell* **2014**, *156*, 317–331.
- (38) Devi, N.; Singh, D.; Honey, M. S.; Chaudhary, S.; Rawal, R. K.; Kumar, V.; Chowdhury, A. K.; Singh, V. In(OTf)₃ catalysed an expeditious synthesis of β -carboline-imidazo[1,2-a]pyridine and imidazo[1,2-a]pyrazine conjugates. *RSC Adv.* **2016**, *6*, 43881–43891.
- (39) Singh, D.; Kumar, V.; Devi, N.; Malakar, C. C.; Shankar, R.; Singh, V. Metal-free decarboxylative amination: an alternative approach towards regioselective synthesis of β -Carboline N-fused imidazoles. *Adv. Synth. Catal.* **2017**, *359*, 1213–1226.
- (40) Brahmabhatt, K. G.; Ahmed, N.; Sabde, S.; Mitra, D.; Singh, I. P.; Bhutani, K. K. Synthesis and evaluation of β -carboline derivatives as inhibitors of human immunodeficiency virus. *Bioorg. Med. Chem. Lett.* **2010**, *20*, 4416–4419.
- (41) Sana, S.; Reddy, V. G.; Bhandari, S.; Reddy, T. S.; Tokala, R.; Sakla, A. P.; Bhargava, S. K.; Shankaraiah, N. Exploration of carbamide derived pyrimidine-thioindole conjugates as potential VEGFR-2 inhibitors with anti-angiogenesis effect. *Eur. J. Med. Chem.* **2020**, *200*, No. 112457.
- (42) Sultana, F.; Reddy Bonam, S.; Reddy, V. G.; Nayak, V. L.; Akunuri, R.; Rani Routhu, S.; Alarifi, A.; Halmuthur, M. S. K.; Kamal, A. Synthesis of benzo[d]imidazo[2,1-b]thiazole-chalcone conjugates as microtubule targeting and apoptosis inducing agents. *Bioorg. Chem.* **2018**, *76*, 1–12.
- (43) Jahan, S.; Ansari, U. A.; Siddiqui, A. J.; Iqbal, D.; Khan, J.; Banawas, S.; Alshehri, B.; Alshahrani, M. M.; Alsagaby, S. A.; Redhu, N. S.; Pant, A. B. Nobiletin ameliorates cellular damage and stress response and restores neuronal identity altered by sodium arsenate exposure in human iPSCs-derived hNPCs. *Pharmaceuticals (Basel, Switzerland)* **2022**, *15*, 593.
- (44) Liu, B.; Wang, H. Oxaliplatin induces ferroptosis and oxidative stress in HT29 colorectal cancer cells by inhibiting the Nrf2 signaling pathway. *Exp. Ther. Med.* **2022**, *23*, 394.
- (45) (a) Parupalli, R.; Akunuri, R.; Spandana, A.; Phanindranath, R.; Pyreddy, S.; Bazaz, M. R.; Vadakattu, M.; Joshi, S. V.; Bujji, S.; Gorre, B.; Yaddanapudi, V. M.; Dandekar, M. P.; Reddy, V. G.; Nagesh, N.; Nanduri, S. Synthesis and biological evaluation of 1-phenyl-4,6-dihydrobenzo[b]pyrazolo[3,4-d]azepin-5(1H)-one/thiones as anticancer agents. *Bioorg. Chem.* **2023**, *135*, No. 106478. (b) Lu, Y.; Zhang, R.; Liu, S.; Zhao, Y.; Gao, J.; Zhu, L. ZT-2S, a new vacuolar H(+)-ATPase inhibitor, induces apoptosis and protective autophagy through ROS generation in HepG2 cells. *Eur. J. Pharmacol.* **2016**, *771*, 130–138.
- (46) Zhu, Y.; Qin, H.; Sun, C.; Shao, B.; Li, G.; Qin, Y.; Kong, D.; Ren, S.; Wang, H.; Wang, Z.; Zhang, J.; Wang, H. Endometrial regenerative cell-derived exosomes attenuate experimental colitis through downregulation of intestine ferroptosis. *Stem Cells Int.* **2022**, *2022*, 3014123.
- (47) Huang, C.; Wen, C.; Yang, M.; Gan, D.; Fan, C.; Li, A.; Li, Q.; Zhao, J.; Zhu, L.; Lu, D. Lycopene protects against t-BHP-induced neuronal oxidative damage and apoptosis via activation of the PI3K/Akt pathway. *Mol. Biol. Rep.* **2019**, *46*, 3387–3397.